15th World Congress on Computational Mechanics (WCCM-XV)
8th Asian Pacific Congress on Computational Mechanics (APCOM-VIII)
Virtual Congress: 31 July – 5 August 2022
S. Koshizuka (Ed.)

MECHANICAL STIMULI IN PREDICTION OF TRABECULAR BONE ADAPTATION: NUMERICAL COMPARISON

EKATERINA SMOTROVA[1], SIMIN LI[1] AND VADIM V. SILBERSCHMIDT[1]*

[1]Wolfson School of Mechanical, Electrical and Manufacturing Engineering, Loughborough University, Loughborough, LE11 3TU, UK, *V.Silberschmidt@lboro.ac.uk, https://www.lboro.ac.uk/departments/meme/staff/vadim-silberschmidt/

Key words: Trabecular bone, Bone adaptation, Bone remodelling

Abstract. *Adaptation is the process, with which bone responds to changes in loading environment and modifies its properties and organisation to meet the mechanical demands. Trabecular bone undergoes significant adaptation when subjected to external forces, accomplished through resorption of old and fractured bone and formation of a new bone material. These processes are assumed to be driven by mechanical stimuli of bone-matrix deformation sensed by bone mechanosensory cells. Although numerous in vivo and in vitro experimental evidence of trabecular bone morphology adaptation was obtained, the exact nature of mechanical stimuli triggering biological responses (i.e., osteoclastic resorption and osteoblastic formation) is still debated. This study aims to compare different mechanical stimuli with regard to their ability to initiate the load-induced adaptation in trabecular bone. For this purpose, a 2D model of two trabeculae, connected at their basement, with bone marrow in the intertrabecular space was developed. The finite-element method was implemented for the model loaded in compression to calculate magnitudes of several candidates of the bone-adaptation stimuli. A user material subroutine was developed to relate a magnitude of each candidate to changes in the shape of trabeculae.*

NOMENCLATURE

BA	Bone adaptation
BR	Bone remodelling
BV/TV	Bone volume fraction
FE	Finite element
ITA	Intertrabecular angle
MPS	Maximum principal strain
SED	Strain energy density
TB	Trabecular bone
Tb.Le	Trabecular length
Tb.Sp	Trabecular separation
Tb.Th	Trabecular thickness
vMS	von Mises stress

1 INTRODUCTION

One of the most important functions of bone is providing a structural support by resisting against the forces of muscle contraction during various motions of the body, against external impacts and gravitational force. Bone tissue is not a petrified structure, as it may appear, but a continuously changing system that adapts its geometrical and mechanical properties in response to changes in external loading environment. This process of functional adaptation is accomplished by cell-mediated *bone remodelling* (BR) – synchronised removal and deposition of a bone material that facilitates rebuilding of bone tissue and ensures the skeleton's ability to withstand mechanical loadings. Trabecular bone (TB) – the porous part of many long, flat and irregular bones – responds to alterations in magnitude and pattern of loading by changing its mechanical properties, spatial organisation and shape. It was found that excessive functional loading results in thickening of individual elements of this bone tissue, *trabeculae*, and aligns trabecular morphology along the lines of principle stress, thus making the trabeculae loaded predominantly in compression or tension [1,2]. This effect is well presented in athletes, as they are often exposed to high-impact dynamic loading conditions [3,4]. While the disuse induces reduction of bone mass, thinning of trabeculae, and deterioration of TB load-bearing capacity [5,6]. This effect is primarily observed in cases of immobilisation and micro-gravity conditions of spaceflight [7,8].

Bone adaptation (BA) to mechanical loadings is hypothesised to be driven by mechanical stimuli sensed by bone mechanosensory cells – osteocytes. Like the neural circuit, osteocytes and their dendritic processes sense stimuli, caused by deformation of a loaded bone matrix, and transmit them from the osteocytes located deep in the bone tissue to the bone surface, thus informing bone-surface cells about a local mechanical condition of the bone [9]. While there is growing evidence of a TB response to alterations in loading environment, the exact nature of a mechanical stimulus triggering load-induced BR activities is currently unknown. This study aims to compare different mechanical signals – von Mises stress (vMS), strain energy density (SED) and maximum principal strain (MPS) – on their ability to trigger load-induced TB adaptation. To achieve this, a 2D model of two trabeculae with the morphological properties corresponding to those of real trabeculae was developed. The finite-element (FE) method was implemented for the model loaded in compression to calculate the magnitudes of vMS, SED and MPS mechanical signals that are widely considered as candidates to trigger the BA [10,11]. Nonuniformity of these signals on the trabecular surface was used to drive a well-established mathematical model of BA that relates the value of a stimulus to bone-formation and -resorption activities. A user material USDFLD subroutine was developed to implement the BA model and redefine the mechanical properties and the shape of trabeculae within a simulation increment.

2 METHODOLOGY

2.1 Bone-adaptation model

The BA algorithm used in this study was based on a mathematical model of Adachi *et al.* [12–14]. This model assumes that remodelling only happens at the bone surface and uses the nonuniformity of a local mechanical signal as a stimulus Γ to trigger BA:

$$\Gamma = \ln(S_i/S_d), \tag{1}$$

where S_i is the value of the signal at the point i on the surface A of trabecula (Figure 1b), S_d is the averaged value of the signal for its neighboring points calculated by

$$S_d = \int_S w(l) S_j dA \Big/ \int_S w(l) dA, \tag{2}$$

where l is the distance between the point i and its neighboring point j, $w(l)$ is the linear decay function of the signal as it is being transmitted within the osteocyte influence distance l_0: $w(l) = 1 - l / l_0$ $(0 \le l < l_0)$.

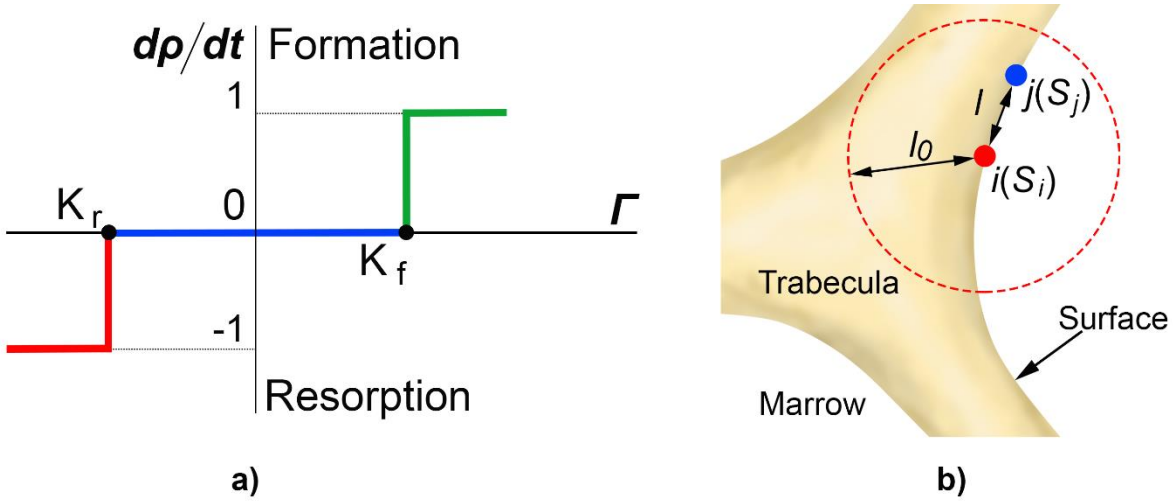

Figure 1: Model of trabecular-bone adaptation driven by mechanical signal S [12]: (a) bone remodelling rate $d\rho/dt$ as function of stimulus Γ: K_r – bone-resorption threshold, K_f – bone-formation threshold. Regions of BR curve: red – resorption due to low stimulus; blue – lazy zone; green – formation due to high stimulus; (b) parameters of bone adaptation model: i – current point at trabecular surface, j – neighbour point at trabecular surface, l – distance between points i and j, l_0 – osteocyte influence distance

A local bone-remodelling rate at the trabecular surface is defined using a step function (Figure 1a) with the following characteristic regions: (i) bone-resorption (K_r) and -formation (K_f) thresholds; (ii) bone resorption when $\Gamma < K_r$; (iii) "lazy zone" corresponding to the absence of BR when $K_r < \Gamma < K_f$; (iv) bone formation when $\Gamma > K_f$. This function is mathematically expressed as:

$$d\rho/dt = \begin{cases} -1 & (\Gamma < K_r), \\ 0 & (K_r < \Gamma < K_f), \\ 1 & (\Gamma > K_f). \end{cases} \tag{3}$$

According to this model, the bone-formation process is represented by recruitment of a marrow element adjacent to the element i to become a bone element. During the resorption process, the element i is converted into a marrow element. The described mathematical model of BA was implemented into a customised USDFLD subroutine that assigned bone or marrow

material properties to a finite element based on the local value of stimulus within a simulation increment. The developed subroutine was used together with Abaqus v.6.20 software (Dassault Systems Simulia Corp, Providence, RI, USA) to carry out the BR process. Parameters of the BA model were set as previously given by Adachi *et al.* [12]: the osteocyte influence distance l_0 was set to 200 μm; the remodelling thresholds K_r and K_f were –0.05 and +0.05, respectively. The nonuniformity of three mechanical signals were used as stimuli to drive this BA model: vMS, SED and MPS. The variants of the BA model with various mechanical signals were denoted Model A (for vMS), Model B (for SED) and Model C (for MPS).

2.2 Analysis domain

In order to compare mechanical signals with regard to their ability to drive BA, a 2D FE model of two trabecula-like elements connected at their basement was developed. Geometrical parameters of the developed FE model were defined by the following parameters: trabecular thickness (Tb.Th), trabecular length (Tb.Le), intertrabecular angle (ITA) and bone volume fraction (BV/TV) (Figure 2).

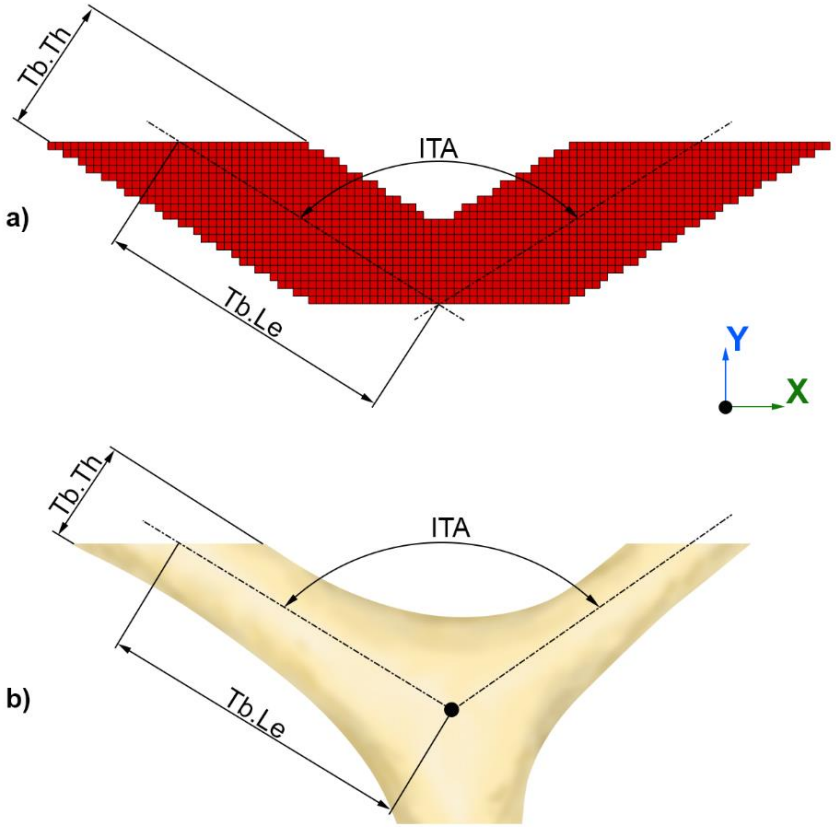

Figure 2: Geometrical parameters of FE model (a) and their relation to morphological parameters of real trabecula (b)

As the microarchitectural parameters for human trabecular bone demonstrate significant

variability for different anatomical locations [15], one anatomical location – femoral head – was selected to set all geometrical parameters of the FE model based on data from the literature (Table 1) [15–18]. The value of ITA – angle between the centrelines of the trabeculae – was set to 116° as it was found to be the mean ITA of nodes with three connecting trabeculae (the most common type of nodes in a femoral head) [18]. The proportion of bone elements in the analysis domain was set to 30 %, based on the reported values of BV/TV for human femoral heads. Two parallel rigid plates were attached at upper and lower surfaces of the FE model using a tie constraint (Figure 3).

Table 1: Geometrical parameters of FE model

Parameter	Value
Trabecular thickness (Tb.Th)	230 μm
Trabecular length (Tb.Le)	500 μm
Intertrabecular angle (ITA)	116°
Bone volume fraction (BV/TV)	30%

2.3 Material properties

Bone was modelled as homogeneous, isotropic, linear-elastic material with the Young's modulus of 15 GPa, corresponding to the stiffness of an individual trabecula measured with nanoindentation [19,20], and the Poisson's ratio of 0.3. Bone marrow – liquidous material that occupies intertrabecular space – was assigned the Young's modulus of 10 kPa and Poisson's ratio of 0.49 [21] in the FE model.

2.4 Loading and boundary conditions

A uniformly distributed compressive load of 3 MPa was applied to the upper rigid plate of the FE model (Figure 3). The load magnitude increased linearly to its maximum value within first 100 increments of the simulation and then remained at that level until the equilibrium of adaptation was reached. Translational degrees of freedom of the lower rigid plate were constrained.

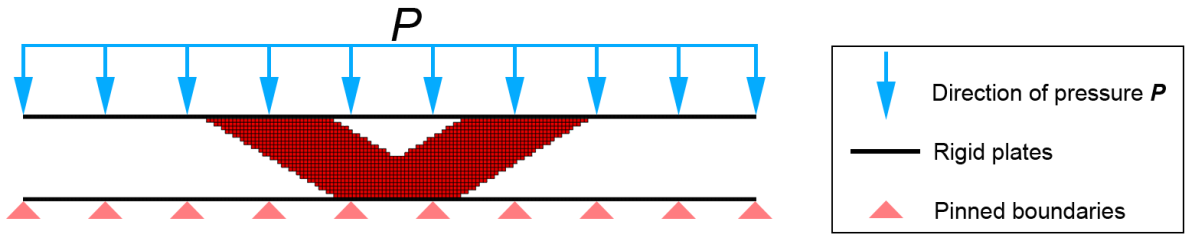

Figure 3: Loading and boundary conditions applied to FE model of trabecular bone

2.5 FE analysis settings

The whole 2500 μm x 265 μm region of simulation was uniformly meshed with 4200 square elements of type CPE4R with the length of 12.5 μm. FE simulations assumed the plane-strain condition and were carried out using Abaqus v.6.20 software.

3 RESULTS AND DISCUSSION

The progress of morphological changes and evolutions of vMS, SED and MPS in the models A, B and C, respectively, due to adaptation to the applied compressive load is presented in Figure 4 for the initial, intermediate and equilibrium states of BA, while Figure 5 illustrates distributions of vMS, SED and MPS at the equilibrium state of BA for all the models. Adaptation was achieved by resorption (conversion of a bone element into a marrow element) and formation (recruitment of a marrow element to become a bone element) of the trabecular surface elements to reduce nonuniformity of the mechanical signal.

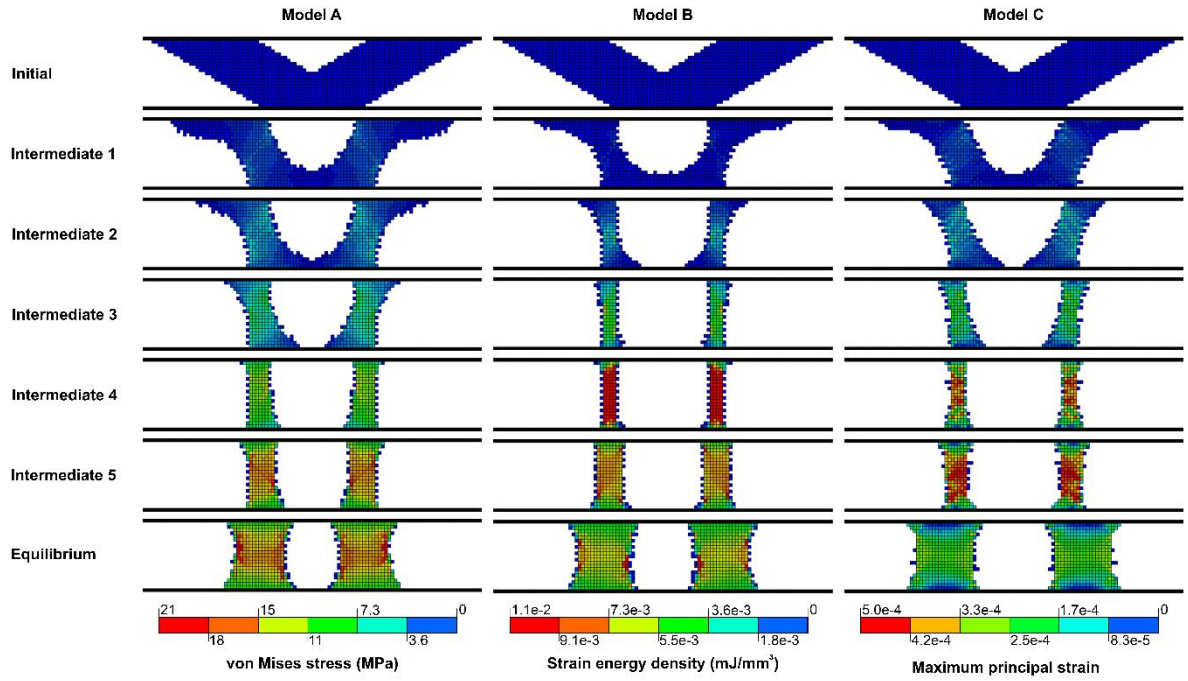

Figure 4: Morphological changes and distributions of von Mises stress, strain energy density and maximum principal strain due to bone adaptation in Models A, B and C

In all the models, the initial V-shaped trabecular geometry was transformed into two parallel columns with wider extremities and a thinner central cross section. The common morphological modifications observed for all the models were the loss of connectivity between the trabeculae, their gradual rotation towards the direction of applied force and cessation of rotation when alignment with the force trajectories was achieved. The BV/TV and Tb.Th morphological parameters demonstrated similar trends for the models, with a rapid initial decrease, a subsequent steep growth of both parameters and reaching a plateau with a stable value (Figure 6). Interestingly, Tb.Th effectively returned to its initial value at the equilibrium state in all models, while BV/TV demonstrated an approximately 35% reduction.

Considering the differences in the obtained results, Model C had a lag in reaching the plateau value of BV/TV and Tb.Th compared with two other models. In addition, Models A and B demonstrated a noticeable movement of trabeculae towards each other, while the equilibrium-state trabeculae of Model C were more separated from each other (Figure 4). To quantify the distance between the trabeculae, trabecular separation (Tb.Sp) was compared

between the top ($\mathrm{Tb.Sp}_t$), central ($\mathrm{Tb.Sp}_c$) and bottom ($\mathrm{Tb.Sp}_b$) regions of the trabeculae. Figure 7 demonstrates that Model A had the smallest Tb.Sp in three analysed regions of trabecula, while Model C had the biggest one for all the regions. Furthermore, Model C exhibited a more uniform distribution of vMS, SED and MPS in the equilibrium stage of adaptation as compared to two other models (Figure 5), which can be explained by a smaller number of single-element protrusions on the surface of trabeculae in this model.

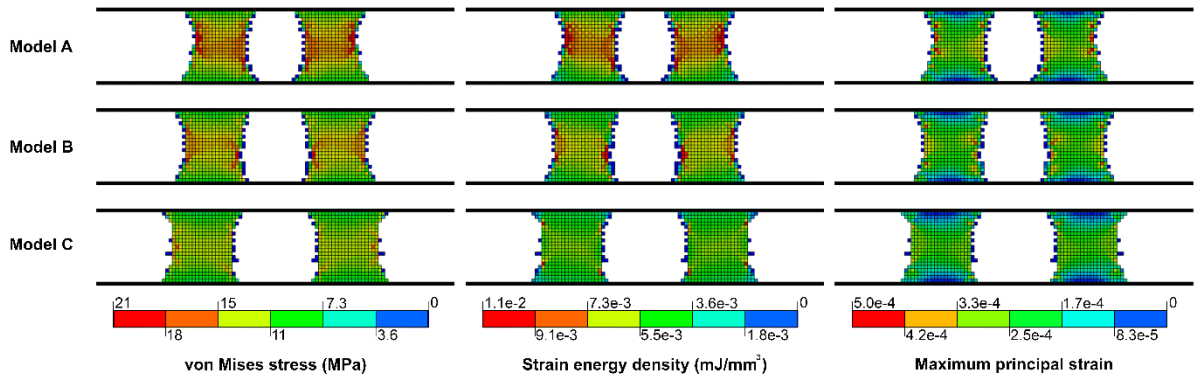

Figure 5: Distribution of von Mises stress, strain energy density and maximum principal strain in post-adaptation equilibrium state in Models A, B and C

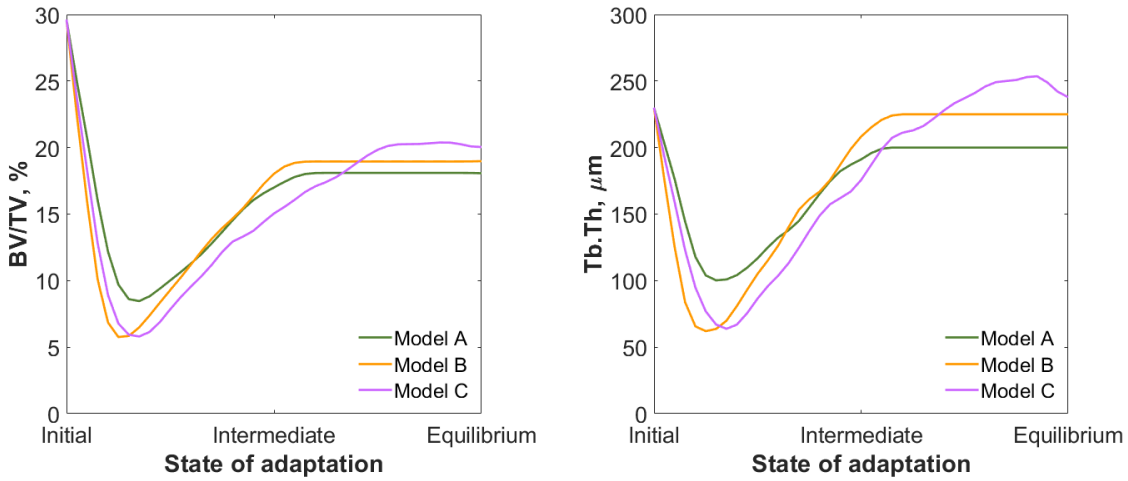

Figure 6: Change of bone volume fraction (BV/TV) and trabecular thickness (Tb.Th) of individual trabecula due to bone adaptation in Models A, B and C

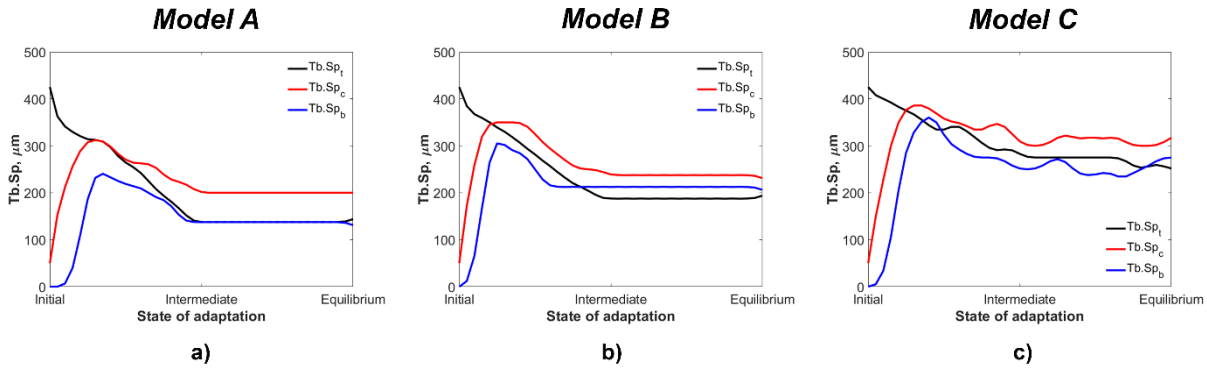

Figure 7: Change of trabecular separation for top ($Tb.Sp_t$), central ($Tb.Sp_c$) and bottom ($Tb.Sp_b$) regions of trabeculae due to bone adaptation in Models A, B and C

REFERENCES

[1] J. Du, C. Hartley, K. Brooke-Wavell, M.A. Paggiosi, J.S. Walsh, S. Li, V. V. Silberschmidt, High-impact exercise stimulated localised adaptation of microarchitecture across distal tibia in postmenopausal women, *Osteoporos. Int.* (2021) **32**:907-919.

[2] T.J. O'leary, S.L. Wardle, R.M. Gifford, R.L. Double, R.M. Reynolds, D.R. Woods, J.P. Greeves, Tibial macrostructure and microarchitecture adaptations in women during 44 weeks of arduous military training, *J. Bone Miner. Res.* (2021) **36**:1300-1315.

[3] J.D. Schipilow, H.M. Macdonald, A.M. Liphardt, M. Kan, S.K. Boyd, Bone micro-architecture, estimated bone strength, and the muscle-bone interaction in elite athletes: an HR-pQCT study, *Bone* (2013) **56**:281-289.

[4] C. Yan, S.G. Moshage, M.E. Kersh, Play during growth: the effect of sports on bone adaptation, *Curr. Osteoporos. Rep.* (2020) **18**:1-12.

[5] M.P. Akhter, G.K. Alvarez, D.M. Cullen, R.R. Recker, Disuse-related decline in trabecular bone structure, *Biomech. Model. Mechanobiol.* (2011) **10**:423-429.

[6] J.F. Yarrow, F. Ye, A. Balaez, J.M. Mantione, D.M. Otzel, C. Chen, L.A. Beggs, C. Baligand, J.E. Keener, W. Lim, R.S. Vohra, Bone loss in a new rodent model combining spinal cord injury and cast immobilization, *J. Musculoskelet. Neuronal Interact.* (2014) **14**:255.

[7] M. Stavnichuk, N. Mikolajewicz, T. Corlett, M. Morris, S.V. Komarova, A systematic review and meta-analysis of bone loss in space travelers, *NPJ Microgravity* (2020) **6**:1-9.

[8] H.E. Berg, O. Eiken, L. Miklavcic, I.B. Mekjavic, Hip, thigh and calf muscle atrophy and bone loss after 5-week bedrest inactivity, *Eur. J. Appl. Physiol.* (2007) **99**:283-289.

[9] T. Adachi, Y. Aonuma, K. Taira, M. Hojo, H. Kamioka, Asymmetric intercellular communication between bone cells: propagation of the calcium signaling, *Biochem. Biophys. Res. Commun.* (2009) **389**:495-500.

[10] K.I. Tsubota, T. Adachi, Simulation study on local and integral mechanical quantities at single trabecular level as candidates of remodeling stimuli, *J. Biomech. Sci. Eng.*

(2006) **1**:124-135.
[11] J. Du, S. Li, V.V. Silberschmidt, Remodelling of trabecular bone in human distal tibia: A model based on an in-vivo HR-pQCT study, *J. Mech. Behav. Biomed. Mater.* (2021) **119**:104506.
[12] T. Adachi, Y. Tomita, H. Sakaue, M. Tanaka, Simulation of trabecular surface remodeling based on local stress nonuniformity, *SME Int. J. Ser. C Mech. Syst. Mach. Elem. Manuf.* (1997) **40**:782-792.
[13] T. Adachi, K.I. Tsubota, Y. Tomita, S.J. Hollister, Trabecular surface remodeling simulation for cancellous bone using microstructural voxel finite element models, *J. Biomech. Eng.* (2001) **123**:403-409.
[14] K.I. Tsubota, T. Adachi, Y. Tomita, Functional adaptation of cancellous bone in human proximal femur predicted by trabecular surface remodeling simulation toward uniform stress state, *J. Biomech.* (2002) **35**:1541-1551.
[15] T. Hildebrand, A. Laib, R. Müller, J. Dequeker, P. Rüegsegger, Direct three-dimensional morphometric analysis of human cancellous bone: microstructural data from spine, femur, iliac crest, and calcaneus, *J. Bone Miner. Res.* (1999) **14**:1167-1174.
[16] N. Reznikov, A.A. Alsheghri, N. Piché, M. Gendron, C. Desrosiers, I. Morozova, J.M.S. Siles, D. Gonzalez-Quevedo, I. Tamimi, J. Song, F. Tamimi, Altered topological blueprint of trabecular bone associates with skeletal pathology in humans, *Bone Reports* (2020) **12**:100264.
[17] Z. He, L. Chu, X. Liu, X. Han, K. Zhang, M. Yan, X. Li, Z. Yu, Differences in subchondral trabecular bone microstructure and finite element analysis-based biomechanical properties between osteoporosis and osteoarthritis, *J. Orthop. Transl.* (2020) **24**:39-45.
[18] N. Reznikov, H. Chase, Y.B. Zvi, V. Tarle, M. Singer, V. Brumfeld, R. Shahar, S. Weiner, Inter-trabecular angle: a parameter of trabecular bone architecture in the human proximal femur that reveals underlying topological motifs, *Acta Biomater.* (2016) **44**:65-72.
[19] J.Y. Rho, T.Y. Tsui, G.M. Pharr, Elastic properties of human cortical and trabecular lamellar bone measured by nanoindentation, Biomater. 18 (1997) 1325–1330.
[20] O. Jiroušek, J. Němeček, D. Kytýř, J. Kunecký, P. Zlamal, T. Doktor, Nanoindentation of trabecular bone-comparison with uniaxial testing of single trabecula, *Chem. List.* (2011) **105**:s668-s671.
[21] L.E. Jansen, N.P. Birch, J.D. Schiffman, A.J. Crosby, S.R. Peyton, Mechanics of intact bone marrow, *J. Mech. Behav. Biomed. Mater.* (2015) **50**:299-307.